RSC Advances

PAPER

View Article Online
View Journal | View Issue

Cite this: *RSC Adv.*, 2021, **11**, 3071

Density functional theory design of double donor dyes and electron transfer on dye/TiO_2(101) composite systems for dye-sensitized solar cells†

Chundan Lin, Yanbing Liu, Di Shao, Guochen Wang, Huiying Xu, Changjin Shao, Wansong Zhang and Zhenqing Yang *

Received 16th October 2020
Accepted 17th December 2020

DOI: 10.1039/d0ra08815c

rsc.li/rsc-advances

In this work, we designed a series of double donor organic dyes, named **ME101–ME106**, based on experimentally synthesized dye **WD8**, and further investigated their electronic structure, the stability of the dye/TiO_2 (101) systems, density of states (DOS) and absorption spectra using density functional theory (DFT) and time-dependent DFT (TDDFT). The molar extinction coefficients of all designed dyes are higher than **WD8**. It's fascinating that **ME106** exhibits a smallest energy gap and 75 nm redshifts compared to **WD8**. The results of calculations reveal that **ME101–ME106**/TiO_2(101) surfaces are more stable than **WD8**, double donor dyes have sufficient electron injection driving force and have very strong transfer electron ability. It is expected that the design of double donors can provide a new understanding and guidance for the investigation of high efficiency dye-sensitized devices.

1. Introduction

Dye sensitized solar cells (DSSCs) have attracted significant interest owing to their high efficiency, easy manufacturing process and their low-cost, and have become one of the most promising photovoltaic devices.[1–7]

DSSCs have a typical sandwich structure, mainly including dye molecules, a metal oxide layer, an electrolyte and a counter electrode. A pivotal component "photosensitizer" is excited by harvesting light and then the conductor band (CB) of TiO_2 accepts the photo-induced electrons with electricity generation. Especially, the sensitizers play a critical role in influencing the photoelectric conversion efficiency (PCE).[8,9] Till now, ruthenium-polypyridyl complexes and metal-free organic dyes have been investigated commonly.[10–13] Conventional Ru-complexes, such as N3/N719 have shown the recorded PCE exceeding 11%,[14–16] and the PCE of zinc porphyrin sensitizers has reached 13%.[17,18] At the same time, more efforts have been turned to design and explore metal-free organic dyes. P. Wang synthesized a new pure organic dye, C281–286, which exhibits high PCE of exceed 13.0%.[19] There are also photosensitizers for colorful and semitransparent dye-sensitized solar cells, which increase its aesthetics while ensuring efficiency.[20–22] And DSSC has effective output power under various lighting conditions, and even has excellent performance under dim conditions, thus paving way for the self-powered indoor light harvesting Internet of Things (IoT) applications.[23–25] These give us more attention to develop more potential organic sensitizers for DSSCs. Up to now, various structures organic dyes are composed of electron donors (D), π-bridges (π) and acceptor moieties (A). At present, there are methods to obtain the PCE of DSSCs with D–π–A structure using only the results from density functional theory (DFT) and time-dependent DFT calculations.[26] In 2019, Zhang *et al.* further explored the molecular structure and internal electron transfer mechanism of TH series dyes (D–A–π–A).[27] In 2008, Ning *et al.* firstly proposed a new D–D–π–A configuration for improving the performance of a DSSC.[28] The additional electron donor in D–D–π–A structure is beneficial not only enhance light absorption capacity, but also inhibit the dye aggregation.[29–31] For example, Dai *et al.* incorporated the **M45** sensitizer based on D–D–π–A form with overall power conversion efficiency of 9.02%.[32] These suggest that D–D–π–A sensitizers will have more brilliant advantages in DSSCs fields.

Dye sensitizers and semiconductor photoanodes are the core of dye-sensitized solar cells. It is important that the individual dye molecule has excellent performance. However, after the dye is adsorbed on TiO_2 surface, the anchoring group will interact with the semiconductor. The excited state electron can be effectively injected into the semiconductor, which is a key process regulating the PCE of the DSSCs. Dye-sensitized solar cells have made great progress, but it is still a difficult problem to accurately investigate the internal electron transfer mechanism of DSSCs. In fact, it turns out to be exertive for giving an in-depth interpretation of the experimental method from the atomic level. Therefore, we use theoretical simulation methods to analyze the electron transfer mechanism. In 2012, Wan *et al.* newly synthesized double electron

Beijing Key Laboratory of Optical Detection Technology for Oil and Gas, College of Science, China University of Petroleum, Beijing 102249, P. R. China. E-mail: yangzhenqing@yahoo.com; yangzhq@cup.edu.cn

† Electronic supplementary information (ESI) available: Optimized geometry structures of **ME101–ME106**, the frontier molecular orbitals of **ME101–ME106** and density of states for **ME101–ME106**. See DOI: 10.1039/d0ra08815c

donor type organic dye **WD8** using phenothiazine as donor group, furan as π-bridge and carboxylic acid as acceptor group.[33] In this work, we designed a range of organic dye **ME101–ME106** by replacing the **WD8**'s donor group in order to seek more promising organic dyes, as shown in Fig. 1. Moreover, we present a systematic investigation on the influence of the dye/TiO_2 on their electronic and optical properties. The geometry of the dye/TiO_2 complex system, electron injection, absorption spectra, and lifetime of the excited state were studied in order to evaluate the performance of the adsorbed systems in DSSCs.

2. Computational methods

All the ground-state geometries were optimized by DFT combined with B3LYP functional in acetonitrile solution with Gaussian 09.[34–37] The excitation states were calculated by CAM-B3LYP/6-31+G*/LanL2DZ for Ti atoms in acetonitrile using conductor like polarizable continuum model (CPCM).[38,39] DFT/DFT+U calculations of dye/TiO_2 were operated on this model using the Vienna *Ab initio* Simulation Package (VASP).[40,41] The Perdew–Burke–Ernzerh (PBE) methods based on generalized gradient-approximation (GGA) were are carried out in all calculations. DFT+U correction is for titanium on the 3d orbital, and the band gap and lattice parameters of TiO_2 were applied: $U = 6$ eV and $J = 0.5$ eV. All methods were believed to access the reliable results compared to the experimental values.[42–44]

3. Results and discussion

3.1 Electronic structure and stability of the dye/TiO_2 (101) system

The excellent performance of the dye molecules depends on individual dye molecules and stability of the dye/TiO_2, which improve photon-to-current conversion efficiency. The structures of **WD8** and **ME101–ME106** were optimized (Fig. S1†), and further energy levels and absorption spectra for **WD8** and **ME101–ME106** were calculated, as shown in Fig. 2 and 3. We can clearly see that the LUMOs of all dyes are higher than the conduction band edge (CBE) of TiO_2 (about −4.0 eV) and HOMOs are lower than the potential (about −4.8 eV) of the I^-/I_3^- redox shuttle.[45] That is to say, these dyes possess enough injection driving force and driving force, so as to ensure the transfer of electrons from the double electron donor to the acceptor (Fig. S2†). In addition, the energy gaps decrease in the sequence of **WD8** > **ME101** > **ME102**> **ME103** > **ME104** > **ME105** > **ME106**, which has a favorable characteristic lead to harvest longer light. From Fig. 3(a), it is obvious that the absorption spectra of the four dyes, **ME101**, **ME102**, **ME105**, and **ME106**, have red-shifts compared to **WD8**, especially maximum

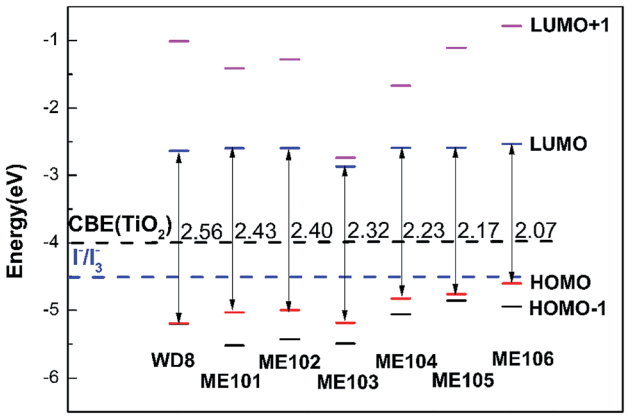

Fig. 2 The energy levels of WD8 and ME101–ME106.

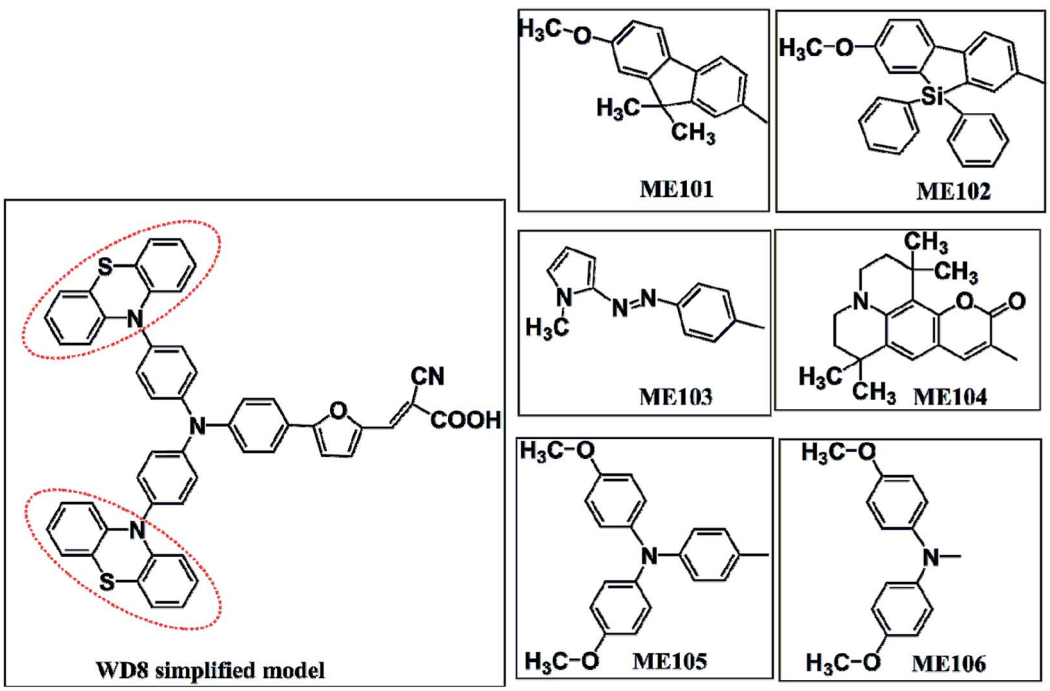

Fig. 1 Molecular structures of dyes WD8 and ME101–ME106.

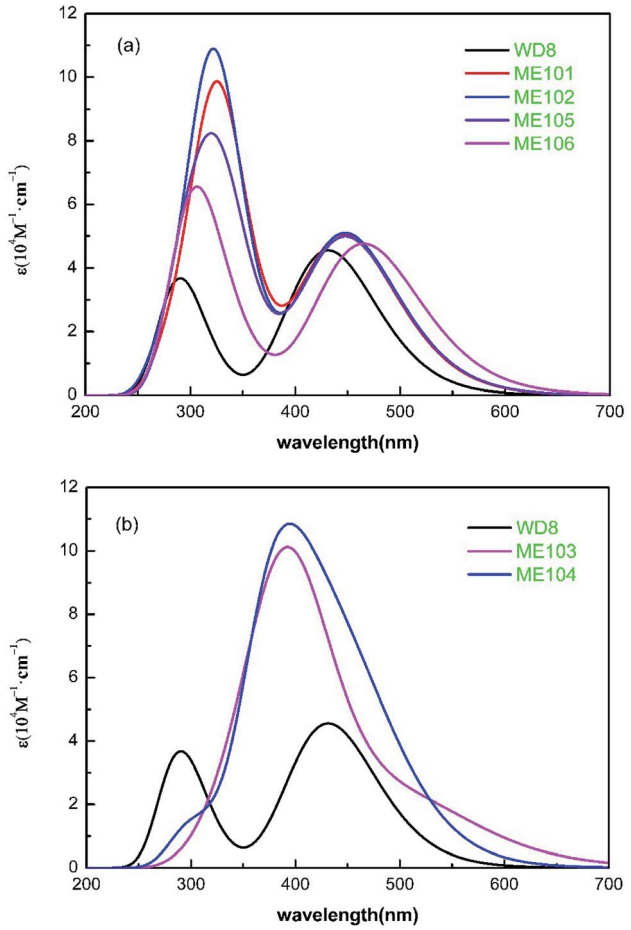

Fig. 3 The calculated UV-visible absorption spectra of all dyes. (a) WD8, ME101, ME102, ME105 and ME106 (b) WD8, ME103 and ME104.

redshifts of **ME106**, which is consistent with the smallest HOMO–LUMO energy gap. From Fig. 3(b), the absorption spectra of **ME103** and **ME104** show a blue shift. The main reason is that the **ME103** molecule contains a nitrogen–nitrogen double bond, which mainly undergoes n–π* transitions, and blue shifts easily occur in the polar solution of acetonitrile. The **ME104** molecule contains –OCO– group, which is also prone to blue shift. Although the **ME103** and **ME104** molecules have only one absorption peak (perhaps because the other absorption peak is weaker, only one absorption peak is displayed), but their molar extinction coefficient increase significantly, the light absorption area of **ME103** and **ME104** are also much larger than that for **WD8**.

After calculation of the isolated dyes, a bidentate chemisorption configuration of the carboxylate of the dye attached to the TiO_2 has been adopted. In other words, the two O atoms of the carboxylic acid in the dye molecules are combined with the Ti atom with a 5-bond to form an O–Ti bond, respectively. The remaining H atoms are attached to the O atom on the corresponding TiO_2 substrate, and the optimized structure of **ME101–ME106**/TiO_2(101) are shown in Fig. 4. As can be seen from the figure, all the dyes are double-donor dye sensitizers and the different electron donor, but all the dye molecules are "T" structures with good verticality. These dyes have a very good planar structure, which facilitates the injection of electrons from the donor to the TiO_2 substrate. We calculated the binding energies of dyes/TiO_2 and the O–Ti bond lengths of the bidentate bridges. The adsorption energy is estimated as: $E_{ads} = E_{slab} + E_{dye} - E_{dye/slab}$, where E_{ads} presents the adsorption energy of the composite system, E_{slab} is the energy of the slab supercell of the TiO_2 anatase (101) surface, E_{dye} is the energy of the sensitizer, and $E_{dye/slab}$ represents the total energy of the dye/TiO_2 (101) composite system. The E_{ads} value is greater than zero, indicating that the bidentate adsorption structure is stable, the larger the E_{ads} value, the more stable adsorption.

3.2 Energy level alignment structure of the dye/TiO_2 (101) system

We theoretically calculated the projected density of states (DOS) for **ME101–ME106**/TiO_2, given in Fig. 5 and S3.† The Fermi level is the energy equaling to zero and other energies are relative to E_f. It can be seen that the calculated HOMO energy levels of all dyes are between the semiconductor conduction band and the valence band (VB), which helps to reduce the band gap of dye-sensitized solar. The narrow band gap promotes the absorption of more long-wavelength light and increases the electron transfer rate at the interface. However, the low energy level of TiO_2 is not beneficial to improve V_{oc}. The LUMO levels of the dyes are all located in the CB of the TiO_2. It is noted that energy level alignment ensures ultrafast interfacial electron injection from the dye to TiO_2 conduction band and reduces the chance of recombination between the injected electrons in CB of TiO_2 and the oxidized dyes. As depicted in Fig. 5 and S3,† the LUMO orbital energy level of **ME101–ME106** dye molecules is higher than that of **WD8**, which the newly designed dye molecules are coupled with TiO_2 conduction band, and also implies the larger injection driving of **ME101–ME106**. Therefore, the dye/semiconductor composite system can effectively transfer and inject electrons, which is expected to improve the performance of DSSCs.

The calculated the energy gaps of isolated dyes **WD8** and **ME101–ME106** are 2.56, 2.43, 2.40, 2.32, 2.23, 2.17, and 2.07 eV, respectively. It is worth noting that when dyes were adsorbed on the surface of TiO_2, the energy gaps of all dye molecules decreased to 1.25, 1.13, 1.10, 1.02, 0.94, 0.87, and 0.77 eV. The results show that when the dyes have been adsorbed, which indicate the same tendency the energy gaps of dyes decrease with the absorption range for the molecules is increased. These findings suggest that changes in the donor group of dye molecules can affect the charge transfer mechanism from the dye to the TiO_2 surface and the energy-level arrangement of the dye/TiO_2 (101) system.

3.3 Absorption spectra of the dye/TiO_2 system

The UV-visible absorption spectra of isolated dye molecules reveal that the newly designed dual-donor dyes have wider absorption spectrum than **WD8** dye, but the HOMO orbital of the dye molecules adsorbed on the TiO_2 substrate changes significantly, which indicates that the dye/TiO_2 system has

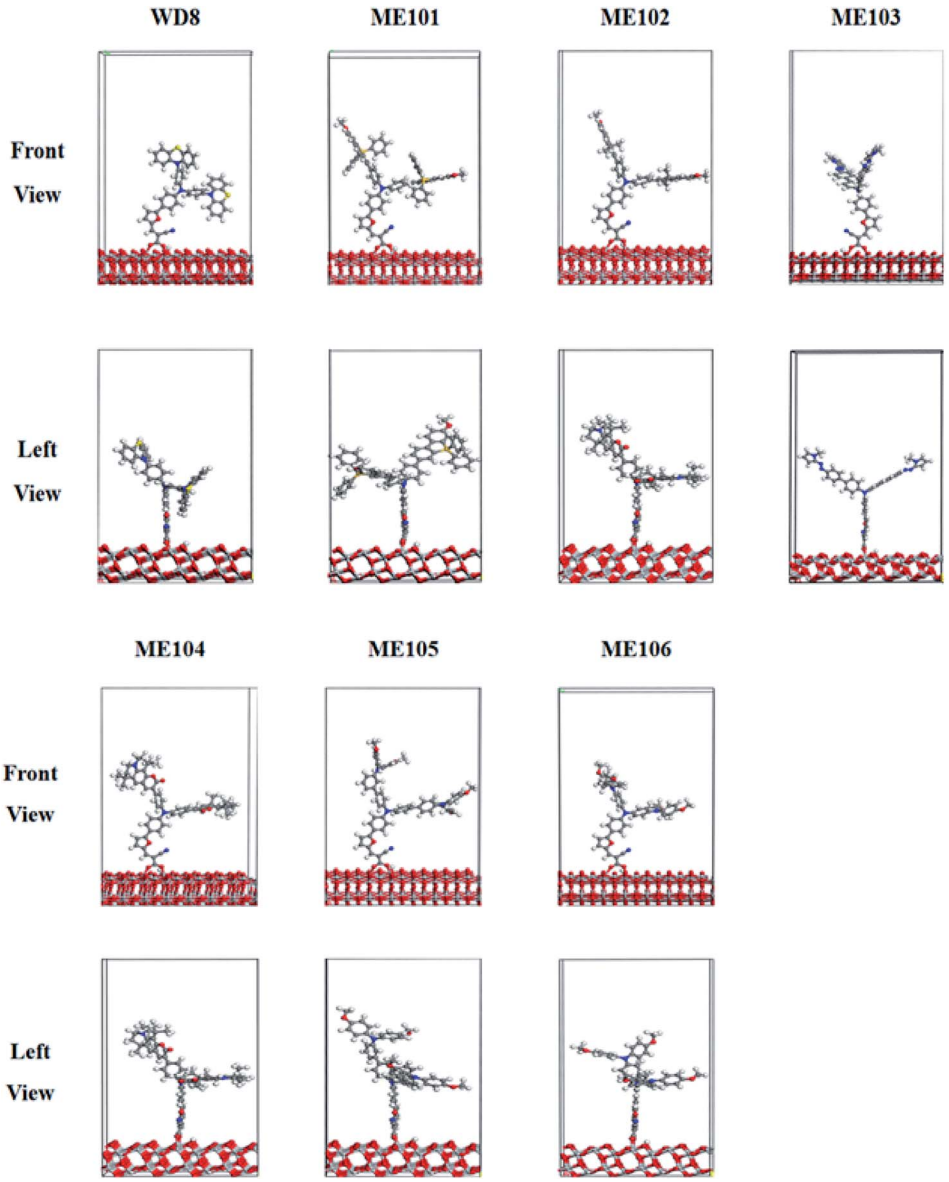

Fig. 4 The configurations of **WD8** and **ME101–ME106** on TiO_2 anatase (101).

a certain impact on UV-visible absorption spectra. In order to verify that the absorption spectrum of adsorbed dyes will be very different from the absorption spectrum of isolated dyes. According to Peng *et al.*[19] recently proposed the model, we consider as a first approximation that the dye is connected to one TiO_2 unit. The binding model is in perfect accordance with the recent results obtained which have demonstrated from infrared spectroscopy analysis in CH_2Cl_2 solution. Therefore, in order to save computing costs, we use the one TiO_2 unit instead of the entire larger TiO_2 substrate to simulate the absorption spectrum of the dye/TiO_2 system. The two O atoms of the anchor group are linked to one Ti atom by a bidentate bonding bridge, with one hydrogen being isolated as one proton on the surface 2c-O atom. The optimized geometry of the dyes **ME106** and **WD8** adsorbing TiO_2 units are shown in Fig. 6. Based on the optimized structure, the excited state of the adsorbed dye was

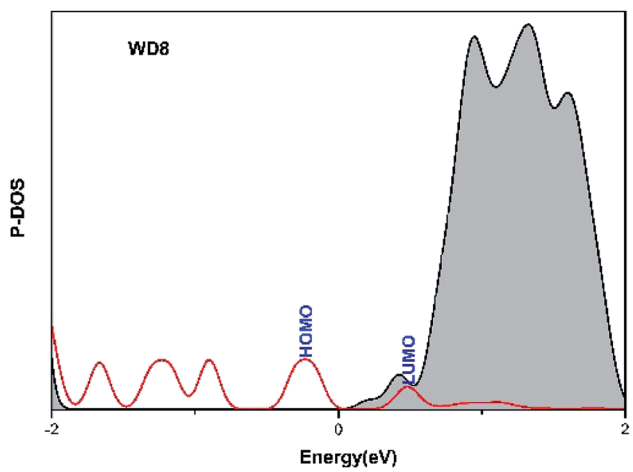

Fig. 5 Calculated projected density of states for **WD8**. Red curves are for the dyes and the black lines are for the TiO_2 substrate.

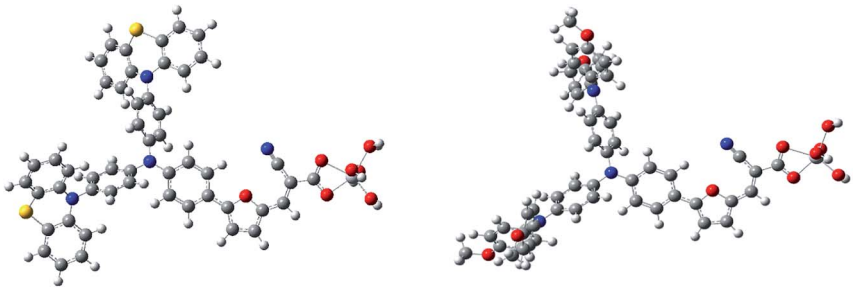

Fig. 6 The geometries of dye **WD8** and **ME106** binding with the minimal TiO_2 cluster.

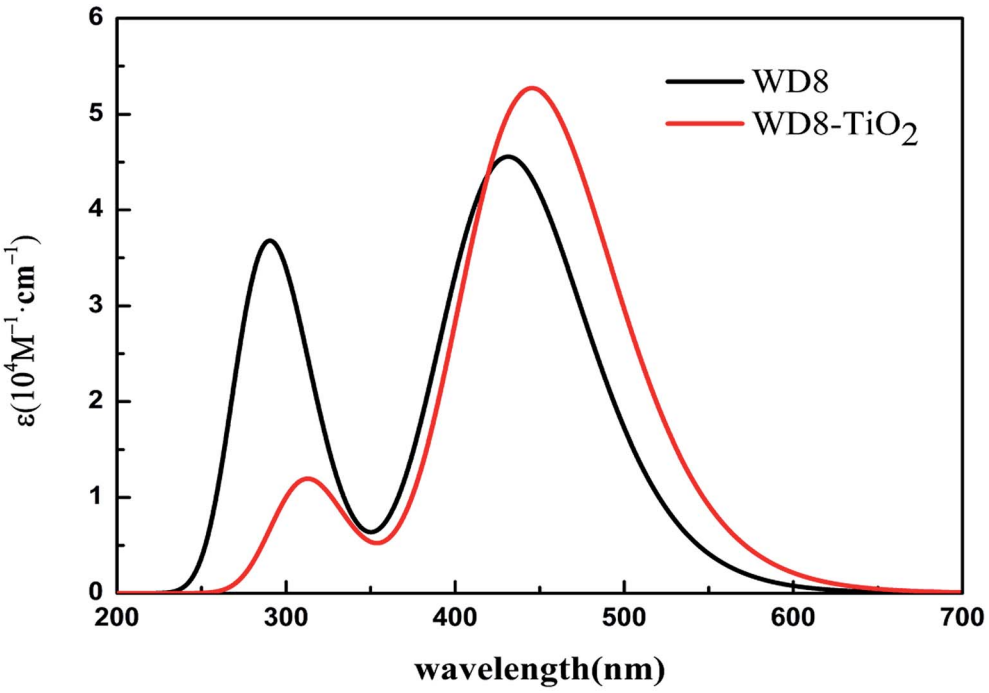

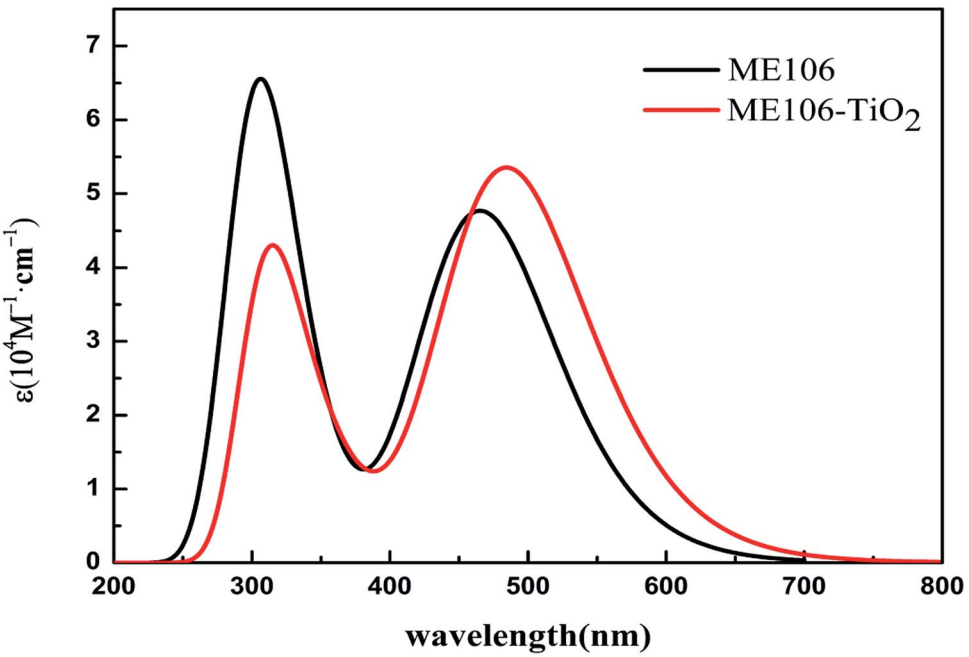

Fig. 7 The UV-visible absorption spectra for isolated dyes and the adsorbed dyes.

calculated by TD-CAM-B3LYP, are presented in Fig. 7. It can be noticed that the absorption spectrum of the adsorbed dye is basically consistent with the absorption spectrum of the isolated dye. There are two absorption peaks, and the main absorption peak of the dye/TiO_2 is superior to isolated dye's, which may be mainly related to the strong interaction between TiO_2 and anchor group of the dye. However, its secondary peak has decreased, which agrees with the transition from π to π^*. The UV-visible absorption spectrum of the dye/TiO_2 is overall red-shifted, owing to the smaller energy gap of the dye/TiO_2, and at the same time, the oscillator strength is also significantly increased. This is a key factor for assessing the photophysical properties of dyes. Therefore, the **ME106** may be theoretically a good candidate as sensitizer of DSSC device.

4. Conclusions

In this work, we present a systematic theoretical study on a new double electron donor organic dyes **ME101–ME106** based on the experimental synthesis organic dye **WD8**. We find that the isolated dyes **ME101–ME106** have the smaller energy gap and the broaden absorption spectrum compared to **WD8**. The calculated results show that **ME101–ME106** possessed more stable adsorption on the TiO_2 surface compared to **WD8**. In addition, the density of states and the absorption spectra of the dye/TiO_2 were calculated by first-principles calculations. Series of characterizations support the roles of the dye/TiO_2 can effectively transfer and inject electrons. The HOMO–LUMO energy gap is reduced and the absorption spectra overall red shift. In theory, **ME101–ME106** may have greater short-circuit photocurrent and open-circuit photovoltage. It is expected that the design of double donors can provide a new strategy and guidance for the investigation in high efficiency dye-sensitized devices.

Conflicts of interest

There are no conflicts to declare.

Acknowledgements

This work is supported by Shanxi Province Science and Technology Major Project (20181101013), the China Scholarship Council Fund (201506445024) and the Higher Education Young Elite Teacher Project (2462015YQ0603) from CUP (China University of Petroleum-Beijing).

References

1 F. Bella, C. Gerbaldi, C. Barolo and M. Grätzel, Aqueous dye-sensitized solar cells, *Chem. Soc. Rev.*, 2015, **44**(44), 3431–3473.

2 A. Hafeldt, G. Boschloo, L. C. Sun, L. Kloo and H. Pettersson, Dye-sensitized solar cells, *Chem. Rev.*, 2010, **110**(110), 6595–6663.

3 B. O'Regan and M. Grätzel, A low-cost, high-efficiency solar cell based on dye-sensitized colloidal TiO_2 films, *Nature*, 1991, **353**, 737–740.

4 J. Baxter and E. Aydil, Nanowire-based dye-sensitized solar cells, *Appl. Phys. Lett.*, 2005, **86**(86), 053114.

5 Y. J. Chang and T. J. Chow, Highly efficient triarylene conjugated dyes for sensitized solar cells, *J. Mater. Chem.*, 2011, **21**(26), 9523–9531.

6 C. H. Huang and Y. J. Chang, Dyes for sensitized solar cells by using [2.2]paracyclophane as a bridging unit, *Tetrahedron Lett.*, 2014, **35**(55), 4938–4942.

7 N. Duvva, Y. K. Eom, G. Reddy, K. S. Schanze and L. Giribabu, Bulky Phenanthroimidazole–Phenothiazine D–π–A Based Organic Sensitizers for Application in Efficient Dye-Sensitized Solar Cells, *ACS Appl. Energy Mater.*, 2020, **3**(7), 6758–6767.

8 A. Mishra, M. K. R. Fischer and P. Bäuerle, Metal-free organic dyes for dye-sensitized solar cells: form structure: property relationships to design rules, *Angew. Chem., Int. Ed.*, 2009, **48**(48), 2474–2499.

9 C. Kim, T. W. Kim, S. Kim, I. Oh, H. Wonneberger, K. Yoon, M. Kwak, J. Kim, J. Kim, C. Li, K. Müllen and H. Ihee, Molecular-Level Understanding of Excited States of N-Annulated Rylene Dye for Dye-Sensitized Solar Cells, *J. Phys. Chem. C*, 2020, **124**(42), 22993–23003.

10 K. Pei, Y. Wu, A. Islam, Q. Zhang, L. Han, H. Tian and W. Zhu, Constructing high-efficiency D–A–π–A-featured solar cell sensitizers: a promising building block of 2,3-diphenylquinoxaline for antiaggregation and photostability, *ACS Appl. Mater. Interfaces*, 2013, **5**(5), 4986–4995.

11 T. Sudyoadsuk, J. Khunchalee, S. Pansay, P. Tongkasee, S. Morada, T. Kaewin, S. Jungsuttiwong and V. Promarak, An organic dye using *N*-dodecyl-3-(3,6-di-*tert*-butylcarbazol-*N*-yl)carbazol-6-yl as a donor moiety for efficient dye-sensitized solar cells, *Tetrahedron Lett.*, 2013, **54**(54), 4903–4907.

12 C. L. Gray, P. Xu, A. J. Rothenberger, S. J. Koehler, E. Elacqua, B. H. Milosavljevic and T. E. Mallouk, Oligomeric Ruthenium Polypyridyl Dye for Improved Stability of Aqueous Photoelectrochemical Cells, *J. Phys. Chem. C*, 2020, **124**(6), 3542–3550.

13 K. T. Mukaddem, P. A. Chater, L. R. Devereux, O. K. Al Bahri, A. Jain and J. M. Cole, Dye-Anchoring Modes at the Dye$\cdots$ TiO_2 Interface of N3- and N749-Sensitized Solar Cells Revealed by Glancing-Angle Pair Distribution Function Analysis, *J. Phys. Chem. C*, 2020, **124**(22), 11935–11945.

14 M. K. Nazeeruddin, P. Pechy and M. Grätzel, Efficient panchromatic sensitization of nanocrystalline TiO_2 films by a black dye based on a trithiocyanato-ruthenium complex, *Chem. Commun.*, 1997, 1705–1706.

15 M. K. Nazeeruddin, A. Kay, I. Rodicio, R. Humphry-Baker, E. Mueller, P. Liska, N. Vlachopoulos and M. Grätzel, Conversion of light to electricity by *cis*-X2bis (2,2′-bipyridyl-4,4′-dicarboxylate)ruthenium(II) charge-transfer sensitizers (X = Cl-, Br-, I-, CN-, and SCN-) on nanocrystalline

titanium dioxide electrodes, *J. Am. Chem. Soc.*, 1993, **115**(115), 6382–6390.

16 K. Portillo-Cortez, *et al.*, N719 Derivatives for Application in a Dye-Sensitized Solar Cell (DSSC): A Theoretical Study, *J. Phys. Chem. A*, 2019, **123**(51), 10930–10939.

17 S. Mathew, A. Yella, P. Gao, R. Humphry-Baker, B. F. Curchod, N. Ashari-Astani, I. Tavernelli, U. Rothlisberger, M. K. Nazeeruddin and M. Gratzel, Dye-sensitized solar cells with 13% efficiency achieved through the molecular engineering of porphyrin sensitizers, *Nat. Chem.*, 2014, **6**(6), 242–247.

18 J.-J. Fu, Y.-A. Duan, J.-Z. Zhang, M.-S. Guo and Y. Liao, Theoretical investigation of novel phenothiazine-based D–π–A conjugated organic dyes as dye-sensitizer in dye-sensitized solar cells, *Theor. Chem.*, 2014, **1045**, 145–153.

19 Z. Yao, H. Wu, Y. Li, J. Wang, J. Zhang, M. Zhang, Y. Guo and P. Wang, Dithienopicenocarbazole as the kernel module of low-energy-gap organic dyes for efficient conversion of sunlight to electricity, *Energy Environ. Sci.*, 2015, **8**(8), 3192–3197.

20 X. R. Xie, D. Y. Sun, Y. F. Wei, Y. Yuan, J. Zhang, Y. T. Ren and P. Wang, Thienochrysenocarbazole based organic dyes for transparent solar cells with over 10% efficiency, *J. Mater. Chem. A*, 2019, **7**(18), 11338–11346.

21 Y. Ren, Y. Cao, D. Zhang, S. M. Zakeeruddin, A. Hagfeldt, P. Wang and M. Grätzel, A Blue Photosensitizer Realizing Efficient and Stable Green Solar Cells via Color Tuning by the Electrolyte, *Adv. Mater.*, 2020, **32**(17), 2000193.

22 H. Wu, J. Zhang, Y. Ren, Y. Zhang, Y. Yuan, Z. Shen, S. Li and P. Wang, Tuning the Color Palette of Semi-Transparent Solar Cells via Lateral π-Extension of Polycyclic Heteroaromatics of Donor–Acceptor Dyes, *ACS Appl. Energy Mater.*, 2020, **3**(5), 4549–4558.

23 A. Aslam, *et al.*, Dye-sensitized solar cells (DSSCs) as a potential photovoltaic technology for the self-powered internet of things (IoTs) applications, *Sol. Energy*, 2020, **207**, 874–892.

24 M. L. Parisi, *et al.*, Prospective life cycle assessment of third-generation photovoltaics at the pre-industrial scale: a long-term scenario approach, *Renewable Sustainable Energy Rev.*, 2020, **121**, 109703.

25 G. Gokul, S. C. Pradhan and S. Soman, Dye-Sensitized Solar Cells as Potential Candidate for Indoor/Diffused Light Harvesting Applications: From BIPV to Self-powered IoTs, in *Advances in Solar Energy Research*, ed. H. Tyagi, A. K. Agarwal, P. R. Chakraborty and S. Powar, Springer Singapore, Singapore, 2019, pp. 281–316.

26 Z. Yang, K. Li, C. Lin, L. R. Devereux, W. Zhang, C. Shao, J. M. Cole and D. Cao, Predicting Device Parameters for Dye-Sensitized Solar Cells from Electronic Structure Calculations to Reproduce Experiment, *ACS Appl. Energy Mater.*, 2020, **3**(5), 4367–4376.

27 J. Jie, Q. Xu, G. Yang, Y. Feng and B. Zhang, Porphyrin sensitizers involving a fluorine-substituted benzothiadiazole as auxiliary acceptor and thiophene as π bridge for use in dye-sensitized solar cells (DSSCs), *Dyes Pigm.*, 2020, **174**, 107984.

28 Z. Ning, Q. Zhang, W. Wu, H. Pei, B. Liu and H. Tian, Starburst triarylamine based dyes for efficient dye-sensitized solar cells, *J. Org. Chem.*, 2008, **73**(73), 3791–3797.

29 S. Wang, H. R. Wang, J. C. Guo, H. B. Tang and J. Z. Zhao, Influence of the terminal electron donor in D–D–π–A phenothiazine dyes for dye-sensitized solar cells, *Dyes Pigm.*, 2014, **109**(109), 96–104.

30 T. Sudyoadsuk, S. Pansay, S. Morada, R. Rattanawan and S. Namuangruk, Synthesis and characterization of D–D–π–A-type organic dyes bearing carbazole–carbazole as a donor moiety (D–D) for efficient dye-sensitized solar, *Eur. J. Org. Chem.*, 2013, **23**(23), 5051–5063.

31 J. K. Roy, S. Kar and J. Leszczynski, Revealing the Photophysical Mechanism of *N*,*N*′-Diphenyl-aniline Based Sensitizers with the D–D–π–A Framework: Theoretical Insights, *ACS Sustainable Chem. Eng.*, 2020, **8**(35), 13328–13341.

32 P. Dai, L. Yang, M. Liang, H. Dong, P. Wang, C. Zhang, Z. Sun and S. Xue, Influence of the terminal electron donor in D–D–π–A organic dye-sensitized solar cells: dithieno[3,2-*b*:2′,3′-*d*] pyrrole versus bis(amine), *ACS Appl. Mater. Interfaces*, 2015, **7**(7), 22436–22447.

33 Z. Wan, C. Jia, Y. Duan, L. Zhou, Y. Lin and Y. Shi, Phenothiazine–triphenylamine based organic dyes containing various conjugated linkers for efficient dye-sensitized solar cells, *J. Mater. Chem.*, 2012, **22**(22), 25140–25147.

34 R. G. Parr, *Density-functional theory of atoms and molecule*, Oxford University Press, 1989, pp. 2592–2598.

35 V. A. Rassolov, M. A. Ratner, J. A. Pople, P. C. Redfern and L. A. Curtiss, 6-31G* basis set for third-row atoms, *J. Comput. Chem.*, 2001, **22**(22), 976–984.

36 M. J. Frisch, G. W. Trucks, H. B. Schlegel, G. E. Scuseria, M. A. Robb, J. R. Cheeseman, G. Scalmani, V. Barone, B. Mennucci, G. A. Petersson, H. Nakatsuji, M. Caricato, X. Li, H. P. Hratchian, A. F. Izmaylov, J. Bloino, G. Zheng, J. L. Sonnenberg, M. Hada, M. Ehara, K. Toyota, R. Fukuda, J. Hasegawa, M. Ishida, T. Nakajima, Y. Honda, O. Kitao, H. Nakai, T. Vreven, J. A. Montgomery Jr, J. E. Peralta, F. Ogliaro, M. Bearpark, J. J. Heyd, E. Brothers, K. N. Kudin, V. N. Staroverov, R. Kobayashi, J. Normand, K. Raghavachari, A. Rendell, J. C. Burant, S. S. Iyengar, J. Tomasi, M. Cossi, N. Rega, J. M. Millam, M. Klene, J. E. Knox, J. B. Cross, V. Bakken, C. Adamo, J. Jaramillo, R. Gomperts, R. E. Stratmann, O. Yazyev, A. J. Austin, R. Cammi, C. Pomelli, J. W. Ochterski, R. L. Martin, K. Morokuma, V. G. Zakrzewski, G. A. Voth, P. Salvador, J. J. Dannenberg, S. Dapprich, A. D. Daniels, O. Farkas, J. B. Foresman, J. V. Ortiz, J. Cioslowski and D. J. Fox, *Gaussian 09, Revision A.1*, Gaussian Inc., Wallingford, CT, 2009.

37 V. Mohankumar, P. Pounraj, M. S. Pandian and P. Ramasamy, Theoretical Investigation on Flavones and Isoflavones-Added Triphenylamine-Based Sensitizers for DSSC Application, *Braz. J. Phys.*, 2019, **49**(1), 103–112.

38 S. Jungsuttiwong, R. Tarsang, T. Sudyoadsuk, V. Promarak, P. Khongpracha and S. Namuangruk, Theoretical study on

novel double donor-based dyes used in high efficient dye-sensitized solar cells: the application of TDDFT study to the electron injection process, *Org. Electron.*, 2013, **14**(3), 711–722.

39 R. Venkatraman, S. V. K. Panneer, E. Varathan and V. Subramanian, Aromaticity–Photovoltaic Property Relationship of Triphenylamine-Based D–π–A Dyes: Leads from DFT Calculations, *J. Phys. Chem. A*, 2020, **124**(17), 3374–3385.

40 S. L. Dudarev, G. A. Botton, S. Y. Savrasov, C. J. Humphreys and A. P. Sutton, Electron energy loss spectra and the structural stability of nickel oxide: an LSDA+U study, *Phys. Rev. B: Condens. Matter Mater. Phys.*, 1998, **57**(9), 1505–1509.

41 G. Kresse and J. Furthmtiller, Efficient iterative schemes for ab initio total-energy calculations using a plane-wave basis set, *Phys. Rev. B: Condens. Matter Mater. Phys.*, 1996, **54**(16), 11169–11186.

42 M. Lazzeri, A. Vittadini and A. Selloni, Erratum: Structure and energetics of stoichiometric TiO_2 anatase surfaces, *Phys. Rev. B: Condens. Matter Mater. Phys.*, 2002, **65**, 119901.

43 W.-L. Ding, D.-M. Wang, Z.-Y. Geng, X.-L. Zhao and Y.-F. Yan, Density functional theory characterization and verification of high-performance indoline dyes with D–A–π–A architecture for dye-sensitized solar cells, *J. Phys. Chem. C*, 2013, **117**, 17382–17398.

44 K. Chaitanya, X.-H. Ju and B. M. Heron, Can elongation of the p-system in triarylamine derived sensitizers with either benzothiadiazole and/or ortho-fluorophenyl moieties enrich their light harvesting efficiency? – a theoretical study, *RSC Adv.*, 2014, **4**, 26621–26634.

45 G. L. Zhang, Y. Bai, R. Z. Li, D. Shi, S. Wenger, S. M. Zakeeruddin, M. Gratzel and P. Wang, Employ a bisthienothiophene linker to construct an organic chromophore for efficient and stable dye-sensitized solar cells, *Energy Environ. Sci.*, 2009, **2**(1), 92–95.